# Enabling the LAAS Differentially Corrected Positioning Service (DCPS): Design and Requirements Alternatives

Young Shin Park, Sam Pullen, and Per Enge, *Stanford University*

## BIOGRAPHIES

Young Shin Park is a Ph.D. Candidate in Aeronautics and Astronautics in the Global Positioning System (GPS) Research Laboratory at Stanford University. Her current research interests are enabling LAAS DCPS, ionospheric anomaly threat model enhancement, and mitigation of the ionospheric anomaly threat to LAAS.

Dr. Sam Pullen is a Senior Research Engineer at Stanford University, where he is the manager of the Local Area Augmentation System (LAAS) research effort. His current work includes the development of revised system architectures and algorithms for the next phase of LAAS to support Category II and III precision landings.

Dr. Per Enge is a Professor of Aeronautics and Astronautics at Stanford University, where he is the Kleiner-Perkins, Mayfield, Sequoia Capital Professor in the School of Engineering. He directs the GPS Research Laboratory at Stanford.

## ABSTRACT

The Local Area Augmentation System (LAAS) can be used for both precision approach and Differentially Corrected Positioning Service (DCPS) applications. Through its support of DCPS, the LAAS Ground Facility (LGF) is required to meet the integrity requirements of all other operations that can receive the LAAS VHF Data Broadcast (VDB). Our previous work demonstrates that the DCPS integrity requirements cannot be met by the existing CAT I LAAS architecture without changes to both the definition of DCPS integrity and the airborne receiver requirements. This paper goes beyond our previous work in identifying the changes that are required and recommending specific sets of alternatives. Because the results of our previous work showed that having the worst-case ionosphere impact to any pair of satellites (as done for precision approach) cannot be supported for DCPS, this work limits the worst-case ionosphere impact to individual satellites. This represents one important but necessary change in the ionosphere anomaly threat model as applied to DCPS. Even with this change, the Maximum Unprotected Error, or MUE, is unacceptably high if no changes to the avionics requirements are made.

Therefore, the results in this paper focus on various combinations of additional aircraft geometry screening and integrity monitoring to lower MUE to a usable level while maintaining useful DCPS availability. Two types of airborne geometry screening rules have been evaluated individually and in combination. The first rule limits airborne subset geometries by numbers of satellites used and the second rule limits the maximum absolute value of the range-to-horizontal-position scalar, $|S_{horizontal}|$. In addition, RAIM is evaluated to obtain additional reduction of MUE. Tables with results for the many alternatives tested are shown.

## 1.0 INTRODUCTION

The Local Area Augmentation System (LAAS) is primarily focused on supporting precision approach but can also be used for a variety of other applications that are known as Differentially Corrected Positioning Service (DCPS) applications. A typical LAAS-equipped airport is illustrated in Figure 1. There are four reference receivers around the LAAS Ground Facility (LGF), which does the central processing and determination of corrections that are transmitted via the VHF Data Broadcast (VDB) antenna. CAT I precision approach availability is typically evaluated at 6 kilometers away from the centroid of the LGF reference receivers, which represents the maximum separation of the CAT I Decision Height (DH) for most airports [7]. Ten nautical miles (18.5 kilometers) farther out along this approach direction marks the boundary of the Precision Approach Region (PAR).

DCPS is broadly composed of (but not limited to) three operations. The first operation is terminal-area navigation for the aircraft in the region from the PAR to 45 kilometers away from the LGF. The second operation is enroute navigation for aircraft passing over the airport that can receive and make use of the LAAS VDB. The third operation is airport surface movement for aircraft on airport taxiways (and thus quite close to the LGF centroid). Note that the VDB is required to provide coverage out to 45 kilometers assuming a 3-degree glideslope for precision approaches. At higher altitudes, aircraft will receive the VDB at significantly further distances.

Through its support of DCPS, the LAAS Ground Facility is required to meet the integrity requirements of all other operations that could use the LAAS VDB. CAT I precision approach is approved under anomalous-ionospheric conditions (the most-constraining threat) for at least a 6-kilometer separation. The current LAAS requirements for DCPS integrity are that position errors should be bounded by the corresponding protection levels to the $10^{-7}$-per-hour probability level, regardless of the size of the error [2,3]. Our previous work [1] demonstrates that the existing DCPS integrity requirements cannot be met by CAT I LAAS without changes to both the definition of DCPS integrity [2,3] and the airborne receiver requirements [4].

This paper goes beyond our previous work in identifying the changes that are required and recommending specific sets of alternatives. To support these decisions, this paper defines specific quality metrics for DCPS analysis. One of these is the “Maximum Unprotected Error”, or “MUE,” which represents the largest error that is not guaranteed to be bounded by the Horizontal Protection Level (HPL) to the $10^{-7}$-per-hour probability level needed for DCPS integrity. This metric quantifies the level of error that DCPS users are allowed to have without violating a revised integrity requirement. The other metric is the projected availability of DCPS for the RTCA-standard 24-satellite constellation [3] with all satellites healthy. In this paper, “availability” represents not only the percentage of available geometries over time but also over all valid subset geometries (including the all-in-view geometry).

Because the results of our previous work showed that having the worst-case ionosphere impact to any pair of satellites (as done for precision approach) cannot be supported for DCPS [1], the DCPS error simulations carried out in this paper limit the worst-case ionosphere impact to individual satellites. This represents one important but necessary change in the ionospheric anomaly threat model as applied to DCPS. Even with this change, the MUE is unacceptably high (roughly 6 kilometers at Memphis) with an effective ionospheric gradient sigma ($\sigma_{vig}$) of 24.1 millimeters per kilometer if no changes to the avionics requirements are made. MUE is even larger (about 350 kilometers) with the nominal $\sigma_{vig}$ of 4 millimeters per kilometer (see Section 4.0 for more details).

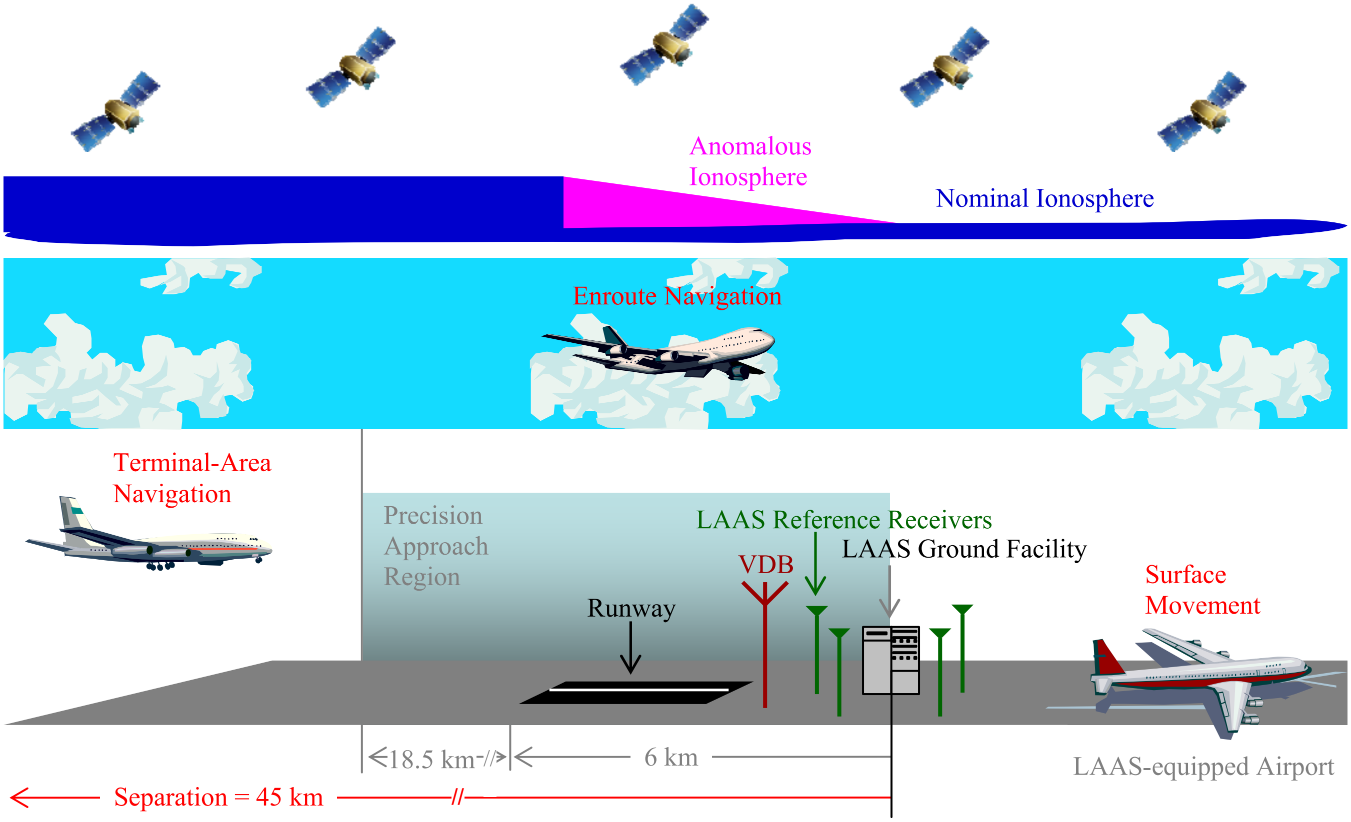

**Figure 1:** Operations Included in DCPS at a LAAS-Equipped Airport.

Therefore, this paper examines various combinations of additional aircraft geometry screening and integrity monitoring. The objective is to minimize MUE so as to maximize the utility of DCPS while maintaining useful availability of the DCPS service.

## 2.0 AIRBORNE GEOMETRY SCREENING RULES

Two types of airborne geometry screening rules have been evaluated individually and in combination. These rules limit valid airborne geometries to (a) no more than $M$ satellites fewer than the $N$ satellites approved by the LGF, where $M \leq 2$ to be helpful since drill-down to 3 satellites out ($M = 3$) has the same MUE as including all usable subset geometries (down to 4 satellites), as demonstrated in [1]; (b) specifying a maximum absolute value of the range-to-position scalar, $|S_{horizontal}|$, that is derived from the weighted pseudoinverse of the user's GPS geometry matrix [4]. The limited subset geometry rule based on (a) has been evaluated in [1]. The second screening rule alone based on (b) and in combination with the limited subset geometry rule is evaluated in this paper. In addition, RAIM using the method in [5] is evaluated to obtain additional reduction of the MUE, although the additional benefit turns out to be relatively small.

## 3.0 SIMULATION PROCEDURE

### *3.1 DCPS SIMULATION OF HPE AND HPL*

The simulation procedure used to analyze DCPS design and requirements alternatives has been expanded from the methodology in [1] and is shown in Figure 2. One day of geometries with a 5-degree mask angle and five-minute time updates from 11 major U.S. airports (including Memphis) is used to generate all-in-view, all 1-satellite-out, all 2-satellites-out, etc., down to all 4-satellite subset geometries, where $N$ represents the number of visible satellites in the geometry (which are all assumed to be approved for use by the LGF). The maximum supported distance from LGF to user, defined as $D_{max}$ and included in the information broadcast by the VDB [4], is nominally set to be 45 kilometers, although shorter maximum separations have also been evaluated.

Worst-case GPS range errors from the ionospheric anomaly threat model for the Conterminous U.S. (CONUS) [6] are applied to all individual satellites in all allowed subset geometries, one satellite at a time. Anomalous ionospheric range errors applied to individual satellites are proportional to the distance from LGF to user with the addition of a bias due to an assumed aircraft velocity of 70 meters per second in the direction of the LGF. This value is used because it is also used for CAT I precision approach, although the actual value for DCPS could be quite different. The nominal ionospheric gradient parameter, $\sigma_{vig}$, varies due to LGF geometry screening to protect CAT I precision approach. Here, the nominal (uninflated) $\sigma_{vig}$ of 4 millimeters per kilometer is used for all screening rules and integrity monitoring. The computed Horizontal Position Error (HPE) and HPL are obtained, and the largest HPE and corresponding HPL are stored for each subset geometry.

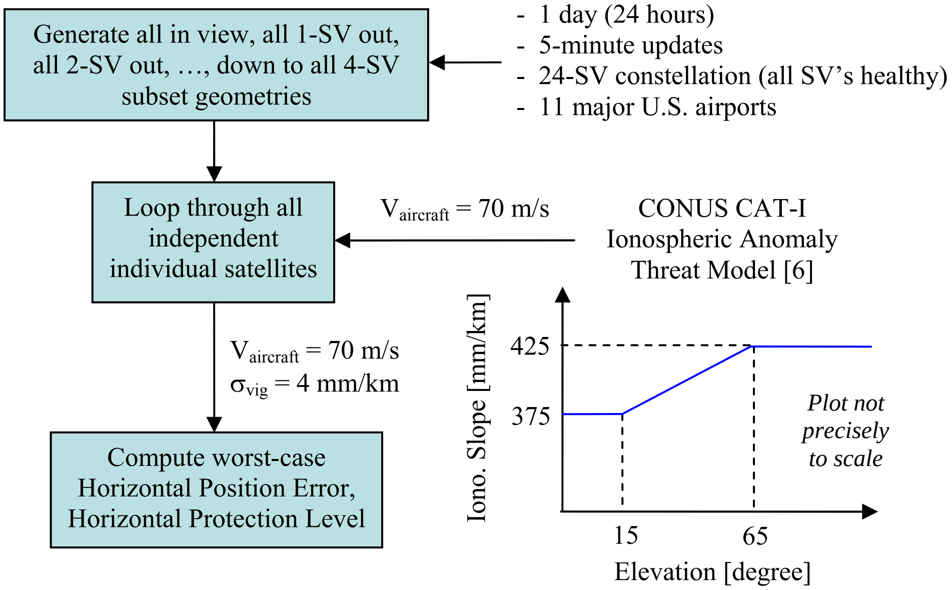

**Figure 2:** DCPS Simulation Procedure to Obtain HPE and HPL.

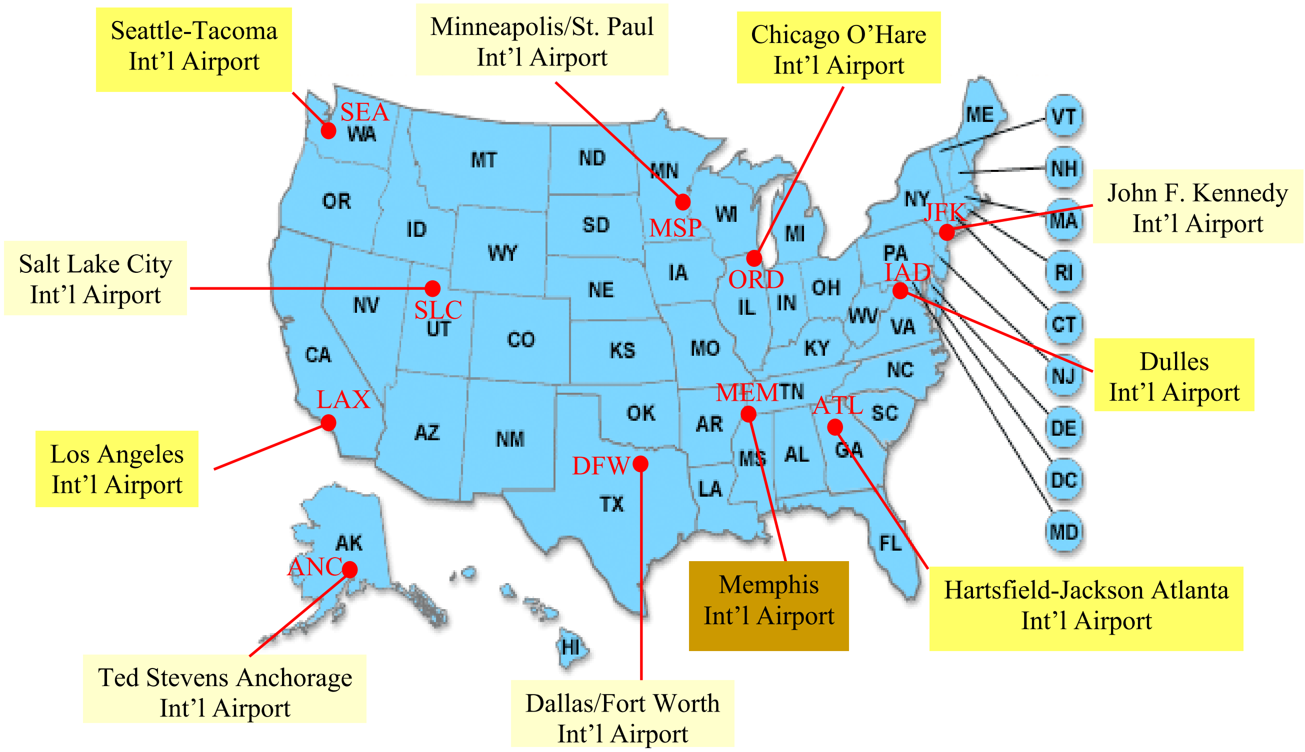

**Figure 3:** Memphis International Airport and Ten Other Major U.S. Airports on Map of U.S. [8].

Eleven (11) major U.S. airports are used to generate GPS satellite geometries: Memphis (MEM), Dulles (IAD), Atlanta (ATL), Chicago O'Hare (ORD), Los Angeles (LAX), Seattle-Tacoma (SEA), New York/John F. Kennedy (JFK), Minneapolis/St. Paul (MSP), Dallas/Fort Worth (DFW), Salt Lake City (SLC), and Anchorage (ANC), as shown in Figure 3. These airports are well-distributed throughout the U.S.

### 3.2 *GEOMETRY SCREENING SIMULATION*

HPE and HPL calculated by the procedure shown in Figure 2 are fed to the geometry screening simulation as inputs. Drill-down to 4-satellite subset geometries is used for geometry screening based on the maximum $|S_{horizontal}|$ limitation rule only, and drill-down to *M*-satellite-out subset geometries is used for geometry screening based on combinations of the maximum $|S_{horizontal}|$ limitation and limited subset geometries, where *M* is less than or equal to two. The geometries whose HPE is not bounded by its HPL (in other words, the HPE-to-HPL ratio exceeds 1.0) are investigated to determine the maximum $|S_{horizontal}|$ needed to protect a certain MUE. Some geometries whose $|S_{horizontal}|$ is greater than the determined maximum $|S_{horizontal}|$ are screened out, and the survived geometries contribute to DCPS availability. For the combinations of airborne geometry screening rules that include RAIM, the maximum $|S_{horizontal}|$ for geometries with 5 or more satellites is determined from the geometries which pass RAIM integrity monitoring for a certain MUE. Since RAIM cannot be used with only 4 satellites, the maximum $|S_{horizontal}|$ value from the combination of the other geometry screening rules is used for 4-satellite geometries. RAIM thresholds are chosen to be values with a $10^{-4}$ probability of false alarm and are listed in Table 1 of [5]. A margin of 10 % is applied to (i.e., subtracted from) the lowest value of maximum $|S_{horizontal}|$ from the several airports simulated to get one maximum $|S_{horizontal}|$ that should cover all airports.

## 4.0 RESULTS AND DISCUSSION

This section presents the results of an example operation. The aircraft in question is making use of DCPS for terminal-area navigation while in the early stages of approach toward a LAAS-equipped airport and is able to receive the VDB while still 45 kilometers away. The aircraft is moving directly toward the airport with a horizontal velocity of 70 meters per second.

As noted in the Introduction, the MUE with no new screening (i.e., as per the current MOPS avionics requirements) is approximately 6 kilometers at Memphis when an inflated (and near-maximum) value of 24.1 millimeters per kilometer is used for $\sigma_{vig}$ and the aircraft velocity in the direction of the LGF is approximately zero.

In this paper, using the nominal $\sigma_{\text{vig}}$ of 4 millimeters per kilometer, the MUE with no new screening (i.e., drill-down to 4-satellite subset geometries) and with an assumed aircraft velocity of 70 meters per second in the direction of the LGF is approximately 350 kilometers at Memphis. The primary reason for this large increase in MUE is that the much lower value of nominal $\sigma_{\text{vig}}$ (compared to the maximum inflated value) greatly reduces HPL, while the worst-case error for each subset geometry remains unchanged.

Figure 4 shows a plot of HPE versus the HPE-to-HPL ratio for various limited subset geometries. Note that all of the horizontal errors on the *y*-axis are significantly larger than the corresponding protection levels. Applying an $N$–2 airborne geometry screening rule, where $M$ is 2, which means the all-in-view, all 1-satellite-out, and all 2-satellites-out subset geometries (only) are considered in the simulation, reduces the MUE to approximately 2.4 kilometers with 99.9% DCPS availability. The MUE is reduced to 89 meters for the $M$ = 1 constraint, and to 30 meters when the airborne geometry screening rule limits subset geometries to only all-in-view geometries.

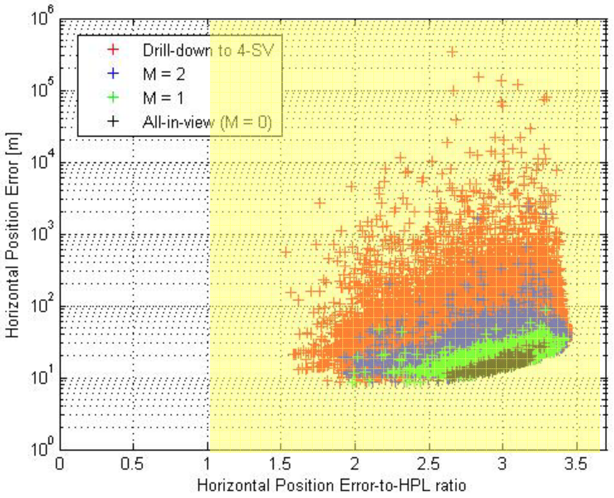

Figure 4: HPE vs. HPE-to-HPL Ratio for Various Limited Subset Geometries

### 4.1 *AIRBORNE GEOMETRY SCREENING BASED ON MAXIMUM $|S_{horizontal}|$ RULE ONLY*

First, airborne geometry screening based on limiting the maximum $|S_{horizontal}|$ only is performed. Because the results from 11 U.S. major airports are similar in terms of availability and maximum $|S_{horizontal}|$, the results from Memphis only are shown in this section (Memphis Int'l. Airport was the first to receive System Design Approval for LAAS precision approach). The values of maximum $|S_{horizontal}|$ are determined using the drill-down to 4-satellite subset geometries from Memphis only. It gives 150 meters of the MUE with approximately 95% DCPS availability with a maximum $|S_{horizontal}|$ of approximately 6.0. Table 1 lists several examples of maximum $|S_{horizontal}|$ and DCPS availability results for MUE values from 150 meters down to 10 meters. As expected, smaller MUE can be achieved with tighter bounds on $|S_{horizontal}|$ and a resulting loss in availability.

**Table 1: Max. $|S_{horizontal}|$, MUE, and DCPS Availability at Memphis Based on Maximum $|S_{horizontal}|$ Only**

| Max. $\lvert S_{horizontal}\rvert$ | MUE (m) | DCPS Availability (%) |
|---|---|---|
| 6.01 | 150 | 95.31 |
| 5.63 | 140 | 94.99 |
| 5.19 | 130 | 94.53 |
| 4.80 | 120 | 94.01 |
| 4.44 | 110 | 93.40 |
| 4.00 | 100 | 92.50 |
| 3.59 | 90 | 91.27 |
| 3.20 | 80 | 89.83 |
| 2.79 | 70 | 87.78 |
| 2.39 | 60 | 84.52 |
| 2.00 | 50 | 78.64 |
| 1.60 | 40 | 68.41 |
| 1.20 | 30 | 51.20 |
| 0.82 | 20 | 22.24 |
| 0.42 | 10 | 0.052 |

The relationship between maximum $|S_{horizontal}|$ and MUE is shown in Figure 5. Reducing the limit on maximum $|S_{horizontal}|$ reduces the screening HAL almost linearly, and this limit can be reduced to the vicinity of 3.0 giving a MUE of approximately 80 meters without unacceptably harming availability down to approximately 90 percent. Recall that "availability" in this context includes all subset geometries down to 4-satellite cases. If availability were instead computed presuming that the aircraft always applied the all-in-view geometry, as is normally done for other applications, the availability would be much higher.

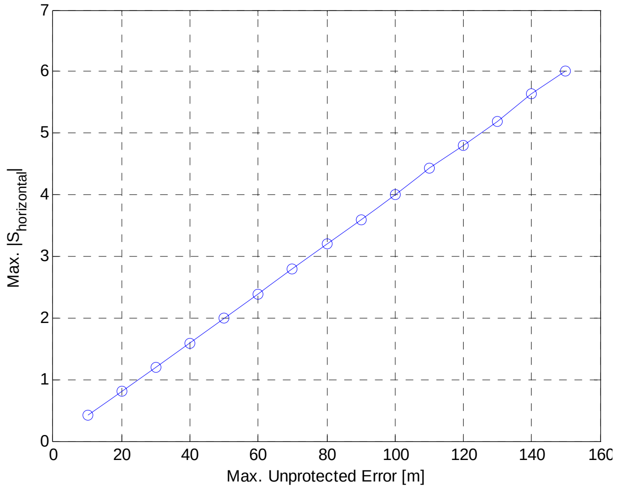

**Figure 5:** Linearity of Maximum $|S_{horizontal}|$ and MUE: Drill-down to 4-satellite Subset Geometries at Memphis.

Note that an MUE of approximately 90 meters, which is supported with 99.9% DCPS availability by applying the limited subset geometry rule ($M = 1$) alone, can be achieved with approximately 91.3% DCPS availability by applying the maximum $|S_{horizontal}|$ rule alone (with a maximum $|S_{horizontal}|$ of 3.59). It makes sense to combine these two screening approaches in an attempt to lower MUE further while maintaining acceptable availability without unduly constraining aircraft subset geometries. The results of this combined approach are shown in the next section.

## *4.2 COMBINATIONS OF AIRBORNE GEOMETRY SCREENING RULES*

Three versions of the limited subset geometry rule are considered for combination with the maximum $|S_{horizontal}|$ rule. These options limit subset geometries to the all-in-view geometry only, to all-in-view plus all 1-satellite-out subsets, and all-in-view, all 1-satellite-out, plus all 2-satellites-out subsets, respectively. All subset geometries must have at least 4 satellites. For this section, the 6 airports highlighted in yellow in Figure 3 are evaluated. It should be noted that the nominal $\sigma_{vig}$ of 4 mm/km is used to evaluate these combinations. When the nominal or minimum value of $\sigma_{vig}$ is broadcast, many more (sometimes most or all) subset geometries have HPE exceeding HPL. Therefore, as with precision approach [6], the primary impact of geometry screening is to lower the maximum HPE for all available subset geometries below MUE. Thus, even though HPE remains unbounded by HPL, these geometries will be acceptable under the proposed revised definition of DCPS integrity.

The maximum $|S_{horizontal}|$ values at these 6 airports for MUE values from 100 meters to 10 meters are listed in Table 2 for the maximum $|S_{horizontal}|$ rule combined with a constraint on subset geometries of $M = 2$, meaning that only subset geometries with 2 or fewer satellites missing from the all-in-view geometry are allowed.

**Table 2: Max. $|S_{horizontal}|$ when Combined with $N$–2 Subset Geometry Limitation at 6 Major U.S. Airports**

| MUE (m) | MEM | IAD | ATL | ORD | LAX | SEA | 10% Margin |
|---|---|---|---|---|---|---|---|
| 100 | 4.13 | 4.20 | 4.10 | 4.05 | 4.07 | 4.06 | 3.65 |
| 90 | 3.68 | 3.67 | 3.69 | 3.74 | 3.62 | 3.67 | 3.26 |
| 80 | 3.41 | 3.28 | 3.26 | 3.26 | 3.25 | 3.21 | 2.89 |
| 70 | 2.81 | 2.82 | 2.89 | 2.81 | 2.84 | 2.83 | 2.53 |
| 60 | 2.42 | 2.42 | 2.40 | 2.40 | 2.42 | 2.43 | 2.16 |
| 50 | 2.00 | 2.00 | 2.01 | 2.01 | 2.01 | 2.02 | 1.80 |
| 40 | 1.60 | 1.60 | 1.61 | 1.60 | 1.60 | 1.61 | 1.44 |
| 30 | 1.20 | 1.20 | 1.20 | 1.20 | 1.20 | 1.20 | 1.08 |
| 20 | 0.80 | 0.80 | 0.80 | 0.80 | 0.80 | 0.80 | 0.72 |
| 10 | 0.41 | 0.41 | 0.42 | 0.43 | 0.42 | 0.42 | 0.37 |

Note that the maximum $|S_{horizontal}|$ over the 6 airports, with 10% margin subtracted to cover airports not simulated here, is given in the far-right-hand column and is used to screen out unprotected geometries for all 6 airports.

The resulting availability for all three combinations of the maximum $|S_{horizontal}|$ rule and subset geometry constraints ($M = 0$, 1, and 2) are shown in Table 3, Table 4, and Table 5, respectively. It is noted that DCPS availability at the 6 different airports are quite similar. When the $M = 0$ constraint is applied, an MUE of 25 meters is achieved with approximately 95% availability. For $M = 1$, the MUE can be reduced to 35 meters with availability greater than 95%. Unfortunately, because typical aircraft maneuvers may occasionally cause tracking of one satellite to be lost, and other causes may remove a second satellite from use, the $M = 2$ constraint is by far the most robust of these options for practical use. As Table 5 shows, an MUE of 50 meters can be supported with 95% or better availability in this case.

**Table 3: DCPS Availability (%) for Max. $|S_{horizontal}|$ with $M = 0$ Subset Geometry Constraint**

| MUE (m) | MEM | IAD | ATL | ORD | LAX | SEA |
|---|---|---|---|---|---|---|
| 100 | 100 | 100 | 100 | 100 | 100 | 100 |
| 90 | 100 | 100 | 100 | 100 | 100 | 100 |
| 80 | 100 | 100 | 100 | 100 | 100 | 100 |
| 70 | 100 | 100 | 100 | 100 | 100 | 100 |
| 60 | 100 | 100 | 100 | 100 | 100 | 100 |
| 50 | 100 | 100 | 100 | 100 | 100 | 100 |
| 40 | 100 | 100 | 100 | 100 | 100 | 100 |
| 30 | 98.61 | 98.96 | 98.61 | 99.65 | 100 | 98.61 |
| 25 | 96.18 | 93.06 | 94.79 | 95.83 | 94.10 | 94.10 |
| 20 | 74.65 | 70.83 | 73.26 | 78.47 | 77.43 | 79.17 |
| 10 | 0.35 | 0.00 | 0.00 | 0.00 | 0.69 | 0.00 |

**Table 4: DCPS Availability (%) for Max. $|S_{horizontal}|$ with $M = 1$ Subset Geometry Constraint**

| MUE (m) | MEM | IAD | ATL | ORD | LAX | SEA |
|---|---|---|---|---|---|---|
| 100 | 100 | 100 | 100 | 100 | 100 | 100 |
| 90 | 100 | 100 | 100 | 100 | 100 | 100 |
| 80 | 99.96 | 100 | 100 | 100 | 100 | 100 |
| 70 | 99.96 | 100 | 100 | 99.92 | 100 | 100 |
| 60 | 99.92 | 100 | 99.96 | 99.88 | 99.92 | 100 |
| 50 | 99.59 | 99.80 | 99.63 | 99.60 | 99.68 | 99.76 |
| 40 | 98.90 | 98.37 | 98.70 | 98.13 | 98.88 | 98.12 |
| 35 | 96.38 | 94.99 | 95.86 | 96.67 | 97.47 | 95.59 |
| 30 | 90.15 | 89.16 | 89.40 | 91.48 | 91.44 | 90.02 |
| 20 | 46.15 | 44.58 | 43.77 | 47.77 | 55.72 | 52.52 |
| 10 | 0.00 | 0.00 | 0.00 | 0.00 | 0.00 | 0.00 |

**Table 5: DCPS Availability (%) for Max. $|S_{horizontal}|$ with $M$ = 2 Subset Geometry Constraint**

| MUE (m) | MEM | IAD | ATL | ORD | LAX | SEA |
|---|---|---|---|---|---|---|
| 100 | 99.35 | 99.22 | 99.21 | 99.38 | 99.12 | 99.43 |
| 90 | 99.20 | 99.02 | 99.07 | 99.18 | 98.95 | 99.22 |
| 80 | 98.98 | 98.74 | 98.78 | 99.00 | 98.70 | 98.85 |
| 70 | 98.46 | 98.22 | 98.45 | 98.63 | 98.20 | 98.51 |
| 60 | 97.54 | 97.12 | 97.51 | 97.63 | 97.39 | 97.82 |
| 50 | 95.64 | 95.16 | 95.47 | 95.53 | 95.83 | 96.01 |
| 40 | 90.55 | 88.70 | 90.07 | 89.65 | 91.88 | 90.73 |
| 30 | 73.51 | 71.35 | 72.76 | 73.80 | 77.82 | 75.34 |
| 20 | 28.38 | 27.58 | 27.13 | 27.20 | 36.34 | 32.21 |
| 10 | 0.00 | 0.00 | 0.00 | 0.00 | 0.00 | 0.00 |

### *4.3 RAIM WITH COMBINATIONS OF AIRBORNE GEOMETRY SCREENING RULES*

RAIM is evaluated in addition to the geometry screening rules shown above because it may already be present in many aircraft that will make use of LAAS DCPS. The addition of RAIM monitoring of large anomalous-ionosphere-induced ranging errors helps relax the maximum $|S_{horizontal}|$ so that better availability can be obtained for the same MUE. The simulation procedure to obtain the maximum $|S_{horizontal}|$ values is different from the previous section because RAIM is added, as described in Section 3.0, while the other algorithms remain the same.

Maximum $|S_{horizontal}|$ values for geometries with 5 or more satellites for the combination of the maximum $|S_{horizontal}|$ rule and the drill-down to 2-satellites-out ($M$ = 2) rule with RAIM are listed in Table 6. Here, some maximum $|S_{horizontal}|$ values are infinite (∞) because no $|S_{horizontal}|$ constraint is needed. This occurs when no horizontal errors exist that exceed HPL or when all such cases are detected by RAIM. RAIM can be used only when the number of satellites in the geometry is at least 5. Therefore, maximum $|S_{horizontal}|$ values determined from combinations of the geometry screening rules without RAIM (derived in the previous section) are used for 4-satellite geometries.

**Table 6: Max. $|S_{horizontal}|$ with RAIM when $N' \geq 5$, $M$ = 2 at 6 Major U.S. Airports**

| MUE (m) | MEM | IAD | ATL | ORD | LAX | SEA | 10% Margin |
|---|---|---|---|---|---|---|---|
| 100 | 4.13 | 4.79 | 4.32 | 4.44 | ∞ | 4.10 | 3.69 |
| 90 | 3.89 | 3.84 | 4.32 | 4.44 | ∞ | 4.10 | 3.46 |
| 80 | 3.67 | 3.71 | 4.32 | 3.26 | 3.25 | 4.10 | 2.92 |
| 70 | 3.58 | 3.00 | 3.27 | 2.85 | 3.25 | 2.97 | 2.57 |
| 60 | 2.60 | 2.53 | 2.63 | 2.63 | 2.42 | 2.47 | 2.18 |
| 50 | 2.05 | 2.07 | 2.01 | 2.07 | 2.02 | 2.09 | 1.81 |
| 40 | 1.61 | 1.60 | 1.65 | 1.66 | 1.64 | 1.62 | 1.44 |
| 30 | 1.23 | 1.23 | 1.21 | 1.22 | 1.21 | 1.21 | 1.09 |
| 20 | 0.83 | 0.83 | 0.85 | 0.80 | 0.83 | 0.88 | 0.72 |
| 10 | 0.58 | 0.56 | 0.63 | 0.59 | 0.70 | 0.59 | 0.50 |

In the same manner as the previous section, DCPS availabilities at 6 airports when RAIM is added to combinations of maximum $|S_{horizontal}|$ and limited subset geometries with $M$ = 0, 1, and 2 are shown in Table 7, Table 8, and Table 9, respectively. Maintaining approximately 95% availability allows MUE to be reduced to below 10 meters for $M$ = 0 (see below), 35 meters for $M$ = 1, and 50 meters for $M$ = 2. Note that the only significant improvement from the results in Section 4.2 is for $M$ = 0 (i.e., use of only the all-in-view geometry). In this case, Table 7 shows that 100% availability is achieved even for an MUE of 10 meters. This is because all errors generated using all-in-view geometries are either bounded by HPL or don't pass RAIM. Therefore, in this unique case, even an MUE of zero meters allows 100 percent DCPS availability, which is another way of saying that the existing DCPS integrity requirement (in which HPL always bounds HPE) can be met for this scenario.

**Table 7: DCPS Availability (%) for RAIM with Max. $|S_{horizontal}|$ and $M$ = 0 Subset Geometry Constraint**

| MUE (m) | MEM | IAD | ATL | ORD | LAX | SEA |
|---|---|---|---|---|---|---|
| 100 | 100 | 100 | 100 | 100 | 100 | 100 |
| 90 | 100 | 100 | 100 | 100 | 100 | 100 |
| 80 | 100 | 100 | 100 | 100 | 100 | 100 |
| 70 | 100 | 100 | 100 | 100 | 100 | 100 |
| 60 | 100 | 100 | 100 | 100 | 100 | 100 |
| 50 | 100 | 100 | 100 | 100 | 100 | 100 |
| 40 | 100 | 100 | 100 | 100 | 100 | 100 |
| 30 | 100 | 100 | 100 | 100 | 100 | 100 |
| 20 | 100 | 100 | 100 | 100 | 100 | 100 |
| 10 | 100 | 100 | 100 | 100 | 100 | 100 |

**Table 8: DCPS Availability (%) for RAIM with Max. $|S_{horizontal}|$ and $M$ = 1 Subset Geometry Constraint**

| MUE (m) | MEM | IAD | ATL | ORD | LAX | SEA |
|---|---|---|---|---|---|---|
| 100 | 100 | 100 | 100 | 100 | 100 | 100 |
| 90 | 100 | 100 | 100 | 100 | 100 | 100 |
| 80 | 99.96 | 100 | 100 | 100 | 100 | 100 |
| 70 | 99.96 | 100 | 100 | 100 | 100 | 100 |
| 60 | 99.96 | 100 | 100 | 100 | 100 | 100 |
| 50 | 99.59 | 99.80 | 99.63 | 99.59 | 99.68 | 99.76 |
| 40 | 98.94 | 98.86 | 99.07 | 98.58 | 99.00 | 98.56 |
| 35 | 96.83 | 95.84 | 96.47 | 97.08 | 97.91 | 96.27 |
| 30 | 90.56 | 89.57 | 89.97 | 91.84 | 91.88 | 90.55 |
| 20 | 59.87 | 57.21 | 58.22 | 60.35 | 66.01 | 64.62 |
| 10 | 14.69 | 14.02 | 14.33 | 13.43 | 23.42 | 18.47 |

**Table 9: DCPS Availability (%) for RAIM with Max. $|S_{horizontal}|$ and $M$ = 2 Subset Geometry Constraint**

| MUE (m) | MEM | IAD | ATL | ORD | LAX | SEA |
|---|---|---|---|---|---|---|
| 100 | 99.37 | 99.22 | 99.24 | 99.38 | 99.12 | 99.44 |
| 90 | 99.25 | 99.01 | 99.12 | 99.28 | 99.01 | 99.29 |
| 80 | 99.00 | 98.77 | 98.80 | 99.01 | 98.74 | 98.85 |
| 70 | 98.51 | 98.26 | 98.46 | 98.68 | 98.23 | 98.56 |
| 60 | 97.58 | 97.22 | 97.57 | 97.68 | 97.43 | 97.88 |
| 50 | 95.70 | 95.21 | 95.55 | 95.63 | 95.88 | 96.19 |
| 40 | 90.68 | 88.83 | 90.16 | 89.76 | 91.96 | 90.80 |
| 30 | 74.12 | 72.19 | 73.52 | 74.68 | 78.45 | 76.06 |
| 20 | 28.54 | 27.83 | 27.25 | 27.37 | 36.58 | 32.38 |
| 10 | 1.58 | 1.67 | 1.11 | 0.82 | 3.18 | 1.93 |

In order to better visualize the improvement in DCPS availability that can be achieved by adding RAIM, the availability for combinations of the screening rules alone and with RAIM are compared in Figure 6 for $M$ = 0, in Figure 7 for $M$ = 1, and in Figure 8 for $M$ = 2. Overall, RAIM appears to be helpful in reducing MUE for the same availability when MUE is less than 30 meters and when subset geometries are limited to fewer satellites missing.

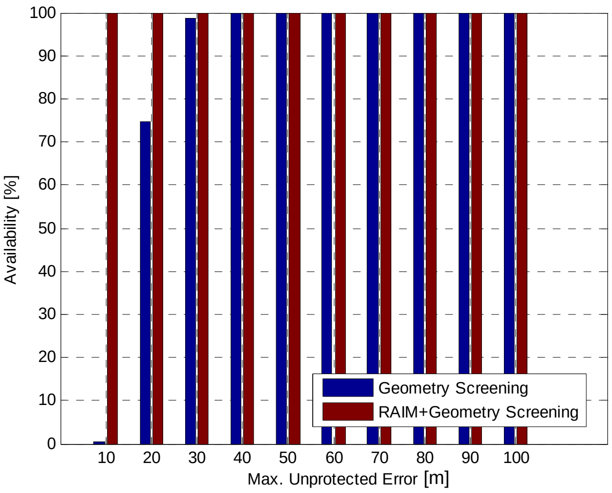

**Figure 6:** Comparison of DCPS Availability between Airborne Geometry Screening alone and with RAIM: Memphis; $M$ = 0.

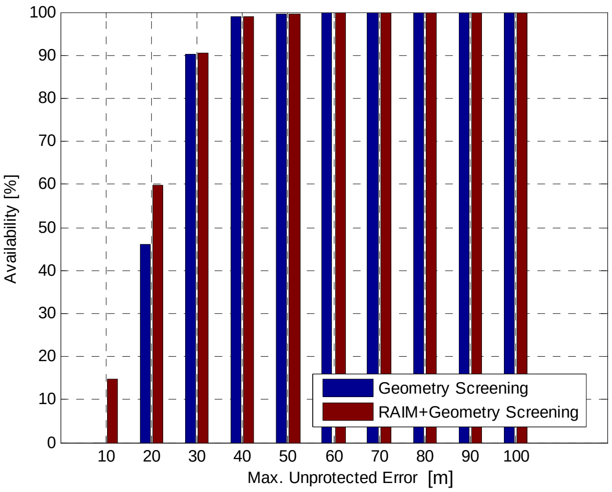

**Figure 7:** Comparison of DCPS Availability between Airborne Geometry Screening alone and with RAIM: Memphis; $M$ = 1.

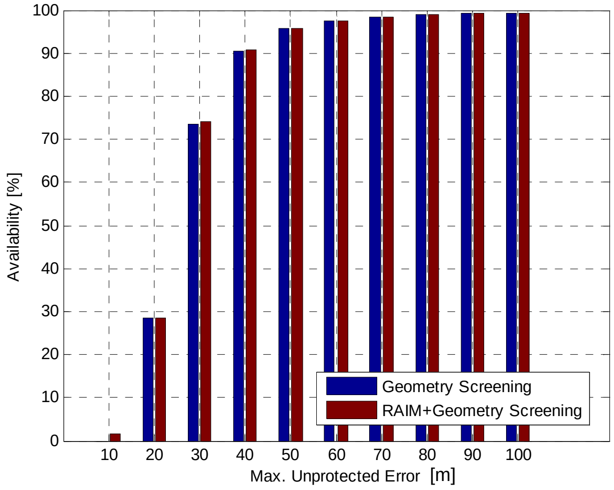

**Figure 8:** Comparison of DCPS Availability between Airborne Geometry Screening alone and with RAIM: Memphis; $M = 2$.

## 5.0 SUMMARY OF RESULTS

To encapsulate the results in this paper, the smallest achievable MUE with more than 95% DCPS availability with a 24-satellite GPS constellation at Memphis, categorized by airborne geometry screening rules and the presence of RAIM, are summarized in Table 10.

**Table 10: Summary of MUE with 95 % Availability: 24-SV Const. at Memphis; $D_{max}$ = 45 km; 1-SV impacted by CONUS Ionosphere Threat Model**

| Airborne Implementation | | MUE | Availability (24 Healthy SV's) |
|---|---|---|---|
| No new screening | | ~ 350 km | > 99.9 % |
| Screening based on 2-satellites-out ($M = 2$) rule only | | 2.4 km | > 99.9 % |
| Screening based on max. $\lvert S_{horizontal} \rvert$ only | | 140 m (max. $\lvert S_{horizontal} \rvert$ = 5.6) | 95.0 % |
| Combinations of $M$ satellite out and max. $\lvert S_{horizontal} \rvert$ | $M = 0$ | 25 m | 96.2 % |
| | $M = 1$ | 35 m | 96.4 % |
| | $M = 2$ | 50 m | 95.6 % |
| RAIM with screening | $M = 0$ | 0 m | > 99.9 % |
| | $M = 1$ | 35 m | 96.8 % |
| | $M = 2$ | 50 m | 95.7 % |

## 6.0 CONCLUSIONS AND FUTURE WORK

Six key conclusions have been drawn from the DCPS analyses conducted in this paper:

(1) Changes to both the DCPS integrity requirements definition and the requirements on LAAS avionics are needed to make DCPS usable.

(2) A change to the impact component of the CONUS LAAS ionospheric anomaly threat model, from 2-satellite to 1-satellite impact, is necessary when this threat model is applied to DCPS.

(3) Once a non-zero value of MUE is allowed by the DCPS integrity requirement, the use of multiple screening rules and, optionally, the use of RAIM for DCPS makes it possible to achieve an MUE for DCPS of about 50 meters (for $D_{max}$ = 45 km) with approximately 95% availability. Further significant reductions do not appear to be possible unless the maximum-gradient bound in the ionospheric anomaly threat model is reduced significantly. However, defining availability more conventionally, in terms of the all-in-view geometries only, would result in significantly lower MUE values at 95% availability.

(4) Because performance differences among the most-helpful options are relatively small, there does not appear to be one clearly "best" choice of additional airborne screening and monitoring. Therefore, the optimal selection depends highly on the specific flight and ground operations to be supported by DCPS and the constraints imposed by existing LAAS airborne equipment.

(5) Because of (3), some future applications of LAAS that planned to use DCPS but would require MUE values of 10 meters or below, such as airport surface movement, may not be supported by DCPS with the CAT I LAAS architecture.

(6) The single-frequency CAT-III LAAS architecture now under development (see [4,7]) will improve DCPS performance by introducing airborne ionospheric-gradient monitoring in addition to airborne geometry screening. However, the additional requirements changes identified in this paper will still be necessary.

Conclusion (5) suggests one important further change to the LAAS avionics requirements. The current LAAS MOPS forbids use of the LAAS Position/Velocity/Timing (PVT) outputs if DCPS is not enabled by the LGF [4]. As this paper points out, even if DCPS is enabled, it will not support all applications that can make use of the PVT outputs. Therefore, the PVT outputs should be "de-linked" from DCPS so that they can be used independently. PVT applications that cannot be supported by DCPS should be defined as separate applications of LAAS in the same manner as precision approach. We suspect that, if airport surface movement is defined as a separate operation, it will probably be supported by the existing LGF geometry screening that mitigates the ionosphere-anomaly threat for CAT I precision approach. Confirming this hypothesis requires a more-intensive study of the requirements on airport surface movement and will be the subject of future work.

## ACKNOWLEDGMENTS

This research was supported by the Federal Aviation Administration (FAA) Local Area Augmentation System (LAAS) Program Office and Stanford Center for Position, Navigation, and Time (SCPNT). Within the FAA, John Warburton and Jason Burns were particularly helpful. The opinions discussed here are those of the authors and do not necessarily represent those of the FAA or SCPNT.

## REFERENCES

[1] Y.S. Park, S. Pullen, and P. Enge, “Mitigation of Anomalous Ionosphere Threat to Enhance Utility of LAAS Differentially Corrected Positioning Service (DCPS),” *Proceedings of IEEE/ION PLANS 2008*, Monterey, CA, May 6-8, 2008.

[2] *Specification: Category I Local Area Augmentation System Ground Facility*. Washington, D.C., Federal Aviation Administration, FAA-E-2937A, April 17, 2002.

[3] *Minimum Aviation System Performance Standards for the Local Area Augmentation System* (*LAAS*), Washington, D.C., RTCA SC-159, WG-4, DO-245A, December 9, 2004.

[4] *Minimum Operational Performance Standards for GPS Local Area Augmentation System Airborne Equipment*. Washington, D.C., RTCA SC-159, WG-4, DO-253C, December 16, 2008.

[5] T. Walter and P. Enge, “Weighted RAIM for Precision Approach,” *Proceedings of ION GPS-95*, Palm Springs, CA, September 12-15, 1995.

[6] S. Pullen, Y.S. Park, and P. Enge, “Impact and Mitigation of Ionospheric Anomalies on Ground Based Augmentation of GNSS,” *Radio Science*, Vol. 44, 2009.

[7] J. Lee, M. Luo, S. Pullen, Y.S. Park, M. Brenner, and P. Enge, “Position-Domain Geometry Screening to Maximize LAAS Availability in the Presence of Ionosphere Anomalies,” *Proceedings of ION GNSS 2006*, Fort Worth, TX, September 26-29 , 2006, pp. 393-408.

[8] U.S map from www.allusairports.com.